Study on the Protective Effect and the Metabolomics Features of Rutaecarpine on Ethanol-induced Acute Gastric Ulcer

sichen ren
Chengdu University of Traditional Chinese Medicine https://orcid.org/0000-0003-0516-1690
Ying Wei
Chengdu University of Traditional Chinese Medicine
Ming Niu
5th Medical Center of Chinese PLA General Hospital
Ruilin Wang
5th Medical Center of Chinese PLA General Hospital
Shizhang Wei
Chengdu University of Traditional Chinese Medicine
Jianxia Wen
Chengdu University of Traditional Chinese Medicine
Dan Wang
Chengdu University of Traditional Chinese Medicine
Tao Yang
Chengdu University of Traditional Chinese Medicine
Xing Chen
Chengdu University of Traditional Chinese Medicine
Shihua Wu
Chengdu University of Traditional Chinese Medicine
Yuling Tong
Chengdu University of Traditional Chinese Medicine
Manyi Jing
5th Medical Center of Chinese PLA General Hospital
Haotian Li
5th Medical Center of Chinese PLA General Hospital
Min Wang
5th Medical Center of Chinese PLA General Hospital
Yanling Zhao (zhaoyl2855@126.com)
5th Medical Center of Chinese PLA General Hospital

Research

Keywords: rutaecarpine, acute gastric ulcer, metabolomics, UPLC-Q-TOF/MS

Posted Date: July 30th, 2020

DOI: https://doi.org/10.21203/rs.3.rs-48441/v1

Abstract

As a prevalent digestive disease, Gastric ulcer (GU) has a high incidence and is seriously harmful to human health. It is an urgent need to finding a natural drug with a gastroprotective effect. Rutaecarpine (RUT) is an alkaloid isolated from *Evodia rutaecarpa* Bentham (Rutaceae). This plant is a traditional Chinese medicine that has been treating gastrointestinal diseases for a long time. The present study aimed to investigate the effects of RUT on ethanol-induced acute GU in mice. After intragastrical administration of RUT for 3 consecutive days, acute GU were induced in the mice by ethanol treatment for 1.5 h. The expression levels of SOD, CAT, NO, ET-1 in serum and EGF, TNF-α, IL-1β, IL-6 in gastric tissues were measured by kits. In addition, hematoxylin and eosin (H&E) staining of gastric mucosa for pathological changes was evaluated. The serum metabolomics method based on ultra-high-performance liquid chromatography combined with quadrupole time-of-flight mass spectrometry (UPLC-Q-TOF/MS) was used to explore the potential mechanism. A total of 7 potential metabolites involved in 9 metabolic pathways were identified. This study helps us to further understand the pathogenesis of GU and provide a potential natural anti-ulcer drug for clinic.

1. Introduction

“Once an ulcer, always an ulcer” is a motto that reveals the characteristics of frequent recurrence and difficult treatment of gastric ulcer in human beings. Gastric ulcer (GU) is a king of superficial diffuse gastric mucosal lesion, which is often caused by excessive drinking and smoking, heavy use of non-steroidal anti-inflammatory drugs (NSAIDs) and serious stress injuries (i.e. shock, surgical injuries and burns). Acute GU can cause severe upper gastrointestinal bleeding, with high morbidity and mortality [1–3]. The main causes for GU formation include *Helicobacter pylori* bacteria infection, gastric hyperacidity, local ischemia or impaired gastric mucosal barrier function [4]. In this study, the mice were selected as the model and absolute ethanol were administered intragastrically to simulate human GUs caused by excessive drinking because the function and anatomical structure of mice's stomach is similar to that of the human stomach. At present, H_2 receptor antagonists, proton pump inhibitors (PPI) and *Helicobacter pylori* eradication therapy are widely applied to the treatment of GU [5]. However, despite their therapeutic effects are satisfactory, there are still some problems such as some associated undesirable adverse drug reactions, high recurrence rate and drug resistance after treatment. Therefore, it is urgent to find a more ideal anti-GU drug. The exploration of natural products may find a more effective, safer and less side-effect alternative .

Rutaecarpine (RUT,Figure 1), a quinazolinocarboline alkaloid extracted from the dried unripe fruit of *Evodia rutaecarpa* Bentham (Rutaceae). This plant is a long-standing Chinese herbal medicine traditionally used for the treat pain, vomiting and pyresis [6]. RUT has a wide range of pharmacological effects, such as cardiovascular protection, improving brain function, protecting gastric mucosa, anti-inflammatory and anti-oxidation. At present, only a few studies have reported that the anti-ulcer effect of RUT may be related to reduction of the asymmetric dimethylarginine (ADMA) by stimulating the release of endogenous calcitonin gene-related peptide (CGRP) via activation of vanilloid receptor in capsaicin-

sensitive sensory nerves [7, 8], and there is no study on the metabolomics characteristics of its anti-ulcer effect.

Metabolomics can characterize the dynamic changes of metabolites throughout the biological system caused by natural fluctuations or response to the environmental factors or external disturbances. Currently, by using the information technology to define these metabolic biomarkers in cells, tissues, organs or biofluids, it can discover the pathway related to the disease process and elucidate the drug mechanism prospectively [9–11].

In the present study, the conventional pharmacology, molecular biology combined with metabolomics strategy based on UPLC-Q-TOF/MS were used to investigate the anti-GU effect of RUT in an ethanol-induced mouse model, and to illustrate the potential biomarkers and related metabolic pathways (Fig. 2). The results could help us to understand the complex pathogenesis of GU and to provide a potential new anti-ulcer strategies and ideas.

2. Materials And Methods

2.1 Reagents

RUT (purity: 98% or more) was purchased from Chengdu Chroma-Biotechnology Company (Chengdu, China). As a positive control, omeprazole magnesium enteric coated tablets (OME) were provided by AstraZeneca Pharmaceutical Co., Ltd. (ground during use, Sweden). Rut and OME were respectively prepared into a solution of 0.5% carboxymethylcellulose sodium (CMC-Na) when used. Kits for epidermal growth factor (EGF), nitric oxide (NO), endothelin-1 (ET-1), tumor necrosis factor-alpha (TNF-α), interleukin-1 Beta (IL-1β),interleukin-6 (IL-6) were provided by Shanghai enzyme linked biology Co., Ltd (Shanghai, China) and superoxide dismutase (SOD), catalase (CAT) were provided by Nanjing Jiancheng Bioengineering Institute (Nanjing, China).

2.2 Animals

50 KM mice, male, SPF grade, weighing 20 ± 2 g, were provided by the SPF (Beijing) Biotechnology Co., Ltd. (animal license No.: SCXK - (Jing) 2019-0010). Mice were maintained in an animal facility under standard laboratory conditions for 1 week prior to the experiments and provided with water and standard chow ad libitum. The room temperature was maintained at 25 °C ± 0.5 °C, and the humidity was maintained at 50% ± 5%. At the same time, the alternating period of light and shade was 12 h/12 h. All animal experiments were approved by the ethics committee of the fifth medical center of the people's Liberation Army General Hospital (approval No.: IACUC-2019-002).

2.3 Induction of gastric ulcer and treatment

After acclimatization for 3 days, Five groups of mice were assigned: (1) control group;(2) ethanol-induced model group; (3) rutaecarpine high dose group (RUT 900 μg/kg); (4) rutaecarpine low dose group (RUT 450 μg/kg); (5) positive control (omeprazole) group (OME 20 mg/kg). Control group and model group

were given 0.5% CMC-Na. After oral administration for 3 days, Mice were restricted from accessing to food for 24 h prior to the last administration. Besides control group,acute gastric ulcer was induced 1 h after the administration via intragastric absolute ethanol administration (0.01 ml/g). Control group were given the same amount of normal saline. 1.5 h after administration of absolute ethanol, the mice were sacrificed. The serum and stomach were collected for further histological and biochemical analyses.

2.4 Gastric ulcer index and inhibition rate

The gastric tissue of mice was taken, cut along the great curvature of the stomach. The chyme was removed, and the stomach was washed slowly and thoroughly with ice normal saline. Then the gastric injury was measured with a vernier caliper, and the gastric ulcer index (UI) was calculated according to the Guth standard [12]: no lesion (score 0), petechial lesion or the lesion < 1 mm (score 1), 1 mm ≤ lesion < 2 mm (score 2), 2 mm ≤ lesion < 3 mm (score 3), 3 mm ≤ lesion < 4 mm (score 4), 4 mm ≤ lesion (score segmentally), and twice for width > 1 mm. The scores were relative values and the mean UI of each group was obtained by dividing the total scores by the number of animals. In addition, further objective characterization of gastric injury, using Image J software (Version 1.8.0; Bethesda, MD, USA) to analyze the area of gastric injury, and calculate the ulcer rate of gastric area.

The ulcer inhibition was calculated as follows:

$$\text{Ulcer inhibition (\%)} = (UI_{\text{model group}} - UI_{\text{administration group}}) / UI_{\text{model group}} \times 100\%$$

The calculation formula of ulcer rate analyzed by Image J software is as follows:

Ulcer rate (%) = area of gastric ulcer / total area of gastric inner surface × 100%

2.5 Evaluation of cytokines in serum and gastric tissues

Levels of SOD, CAT, NO, ET-1 in serum and EGF, TNF-α, IL-1β, IL-6 in the gastric tissues homogenate of different treated groups were measured according to the instructions provided by the manufacturer.

2.6 Histological and immunohistochemical analysis

The gastric tissues were taken from the same position in general tissue and fix in 10% buffered formalin for more than 48 h. After dehydrating in graded alcohol and embedding in paraffin wax, the sections were cut to a thickness of 4 μm and stained with hematoxylin and eosin (H&E) for histological evaluation. Then the pathological changes in the gastric tissues were observed under a light microscope.

2.7 Serum sample handling

Briefly, 200 μl of thawed serum and 600 μl of methanol were transferred to a 1.5 ml polypropylene tube and mixed uniformly. Then the samples were allowed to stand for 20 min at 4 °C before use and centrifuged at 12000 rpm at 4 °C for 10 min to remove the solid debris. Finally, the supernatant was obtained and filtered through a micropore filter (0.22 μm) to obtain the sample for analysis.

2.8 Chromatography and Mass Spectrometry

An Agilent 6550 iFunnel Q-TOF LC/MS system (Agilent Technologies, Santa Clara, CA, USA) and a ZORBAX RRHD 300 SB-C18 column (2.1 mm i.d. × 100 mm, 1.8 μm i.d., Agilent Technologies, USA) were used for chromatography and separation. 4 μL aliquots of each sample was injected into the column in random order. The column temperature was maintained at 30 °C. The mobile phase was composed of solvent A (water with 0.1% formic acid) and solvent B (acetonitrile with 0.1% formic acid), which was used for a linear gradient separation at a flow rate of 0.30 mL/min for 25 minutes. The gradient was set as follows: 100% A over initial to 1 min, 100–60% A from 1 to 9 min, 60–10% A from 9 to 19 min, 10–0% A from 19 to 21 min and 100% B from 21 to 25 min. To ensure the repeatability and stability of UHPLC-Q-TOF/MS system. Both positive and negative mode electrospray ionization sources (ESI) were used. The electrospray capillary voltage was 4.0 kV in positive ionization mode and 3.0 kV in negative ionization mode. The gas temperature was set at 225 °C and the gas flow rate was 13 L/min. The sheath gas temperature was set at 275 °C and the sheath gas flow was 12 L/min. The nebulizer was set to 20 psi. The mass scan range was set from 80 to 1000 m/z. The nozzle voltage was 2000 V in both negative and positive modes.

2.9 Data processing and multivariate analysis

MassHunter Profinder (version B.06.00; Agilent, CA, USA) was used to process sample and perform peak detection and alignment. The full scan mode was applied to the mass range of 80–1000 m/z and the initial and final retention times were set for data collection. The data filtering and normalization were accomplished by the MetaboAnalyst 4.0 online software (http://www.metaboanalyst.ca), and then introduce the resultant data matrix into SIMCA-P software (version 14.1; Umetrics, Umea, Sweden) for multivariate analysis including principal component analysis (PCA) and orthogonal projection to latent structures discriminate analysis (OPLS-DA). The differential metabolites satisfying the conditions (VIP > 1 and |P(corr)| ≥ 0.58) in the OPLS-DA analysis were selected as potential biomarkers [13].

2.10 Potential biomarkers identification and pathway enrichment analysis

Metabolites satisfying the conditions ($P < 0.05$ and folder change value > 2) among groups calculated by MetaboAnalyst 4.0 software (http://www.MetaboAnalyst.ca/) were selected as potential metabolites. All metabolites (molecular weight error < 20 ppm) were tentatively identified based on the accurate mass charge ratio using the online biochemical database HMDB database (http://www.hmdb.ca/) and METLIN (http://metlin.scripps.edu/). The identified compounds were resubmitted to MetaboAnalyst 4.0 to analyst the signaling pathways based on the pathway library of mus musculus.

2.11 Statistical analysis

All data were expressed as mean ± standard deviation (SD). The differences between groups were compared by one-way ANOVA and two groups were compared by t-test using SPSS software (version 24.0; Chicago, IL, USA). $P < 0.05$ was regarded as statistically significant, and $P < 0.01$ was regarded as highly statistically significant.

3. Results

3.1. Effect of RUT on gastric lesions induced by ethanol

The signs of macroscopic damage were examined to explore the severity of GU. Intragastric administration of absolute ethanol triggered several linear hemorrhagic damage and multifocal erosions compared to the control group (Fig. 3A, B). Compared with the model group, the degree of injury in the treatment group was improved evidently (Fig. 3C, D, E).

3.2. Effect of RUT on ulcer index and inhibition rate

Guth scoring method was used to score the gastric ulcer index in the administration group decreased to different degrees (Table 1). Compared with the model group, the OME 20 mg/kg group, the RUT 450 μg/kg and the RUT can obviously inhibit the GU induced by absolute ethanol ($P < 0.01$). Among them, the 900 μg/kg group had the lowest injury degree and the highest ulcer inhibition rate (60.14%).

Table 1
Effect of RUT on ulcer index and inhibition rate

group	ulcer index	inhibition rate
Control	0	—
Model	$54.25 \pm 5.230^{\#\#}$	—
RUT 450 μg/kg	$33.88 \pm 2.475^{**}$	37.56%
RUT 900 μg/kg	$21.63 \pm 1.847^{**}$	60.14%
OME 20 mg/kg	$26.50 \pm 3.024^{**}$	51.15%

Results expressed as mean ± standard deviation (n = 8). $^{\#}P < 0.05$, $^{\#\#}P < 0.01$ when compared with the control group; $^{*}P < 0.05$, $^{**}P < 0.01$ when compared with the model group.

In order to further objectively characterize the gastric injury in mice, the area of GU in the photos was processed by Image J analysis software, the results were shown in Fig. 3F, and the trend was consistent with Guth score.

3.3 Effect of RUT on cytokines in serum and gastric tissues.

In order to explore the protective effect of RUT on ethanol-induced gastric mucosal damage, we measured the levels of EGF, oxidative stress biomarkers SOD, CAT, NO and inflammatory factors ET-1, TNF-α, IL-1β and IL-6 (Fig. 4). Oral administration of ethanol caused significant increase in the levels of the ET-1 in serum, TNF-α, IL-1β, IL-6 in gastric tissues and suppressed the activity of EGF in gastric tissues, SOD, CAT, NO in serum as compared with those in control group ($P < 0.01$). Pretreatment with RUT or OME reversed the aboved changes as compared with model group ($P < 0.05$ or < 0.01).

Figure 4. The effects of RUT on SOD, CAT, ET-1, NO in serum and ET-1, TNF-α, IL-1β, IL-6 in gastric tissue. Results expressed as mean ± standard deviation (n = 6). A: superoxide dismutase (SOD); B: catalase (CAT); C: endothelin-1 (ET-1); D: nitric oxide (NO); E: epidermal growth factor (EGF); F: tumor necrosis factor-alpha (TNF-α); G: interleukin-1 Beta (IL-1β); H: interleukin-6 (IL-6). $^{\#}P<0.05$, $^{\#\#}P<0.01$ when compared with the control group; $^{*}P<0.05$, $^{**}P<0.01$ when compared with the model group.

3.4 Histopathological examination of gastric tissues

Gastric sections from control group displayed an intact architecture of the gastric wall in the mucosa. In contrast, administration of ethanol triggered a severe gastric injury characterized by hemorrhagic injury, submucosal edema, inflammatory cell infiltration and epithelial cell loss (Fig. 5). Pretreatment with RUT (900 μg/kg, 450 μg/kg) and 20 mg/kg OME attenuated ethanol-induced pathological changes.

3.5 Multivariate statistical analysis and potential biomarkers exploring

Principal component analysis (PCA) is a dimension–reduction statistical method that transfers a set of possibly correlated variables to linear uncorrelated variables (i.e. principal components) by orthogonal transformation [14]. Score plot revealed a direct image of observational clusters. In this study, SIMCA-14.1 software was used to study the metabolome differences between the control, model and 900 μg/kg groups in the serum metabolome by PCA. As seen in Fig. 6, a significant classification between the clustering of the control, model groups and 900 μg/kg RUT groups was observed intuitively in both the ESI + and ESI − modes, which indicated the significant difference in these groups.

Orthogonal partial least squares discriminant analysis (OPLS-DA), as a pattern recognition approach, combines and improves partial least squares (PLS) and orthogonal signal correction (OSC). It could only be used for screening differentially expressed metabolites between the two groups. This present study aimed to explore the specific metabolites regulated by RUT in mice with GU. Therefore, we respectively indentified differential metabolites from the control vs model groups and the model vs 800 μg/kg RUT groups in OPLS-DA mode. R2X (cum), R2Y (cum) and Q2 (cum) were used to estimate how well the model fits the data. As shown in Fig. 8, there was a statistically biochemical perturbation among the clustering of the control, model and 800 μg/kg RUT both in ESI+ (Fig. 7A, D) and ESI- (Fig. 7G, J) models. The relevant parameter above showed that both the positive and negative models had good quality and accurate prediction characteristics. In addition, we used S-plots (Fig. 7B, E, H, K) and permutation tests (n = 100, Fig. 7C, F, I, L) to further validate the models. These permutation tests compared the goodness of fit of the original models with the randomly permuted models, and in the corresponding S-plot, variables whose P(corr) absolute values were over 0.58 and VIP value were over 1 at average means can be regarded as potential biomarkers.

Figure 7. The OPLS-DA score plots, S-plots and 100-permutation test generated from the OPLS-DA data of the control, model and RUT 900 μg/kg groups. OPLS-DA score plots were the pair-wise comparisons in ESI + mode, control vs model group (A), model vs RUT 900 μg/kg group (D) as well as in ESI- mode,

control vs model group (G), model vs RUT 900 μg/kg group (J); S-plots of the OPLS-DA model in ESI + mode, control vs model group (B), model vs RUT 900 μg/kg group (E) as well as in ESI- mode, control vs model group (H), model vs RUT 900 μg/kg group (K). The 100-permutation test of the OPLS-DA model in ESI + mode, control vs model group (C), model vs RUT 900 μg/kg group (F) as well as in ESI- mode, control vs model group (I), model vs RUT 900 μg/kg group (L).

3.6 Potential metabolites in the treatment of GU

To characterize differential metabolites more comprehensively, the potential differential metabolites obtained under ESI + and ESI − modes were combined for subsequent analysis. There were 3304 signals detected in the control, model and 900 μg/kg RUT groups. Based on the threshold of VIP > 1.0 and |P(corr)| ≥ 0.58, potential differential metabolites that have substantially contributed to the clustering and discrimination were selected for ANOVA analysis. Then METLIN and Metaboanalyst databases were used to identified candidates with significant changes as biomarkers. Finally, 7 potential biomarkers were identified, 6 in ESI- mode and 1 in ESI + mode. These metabolites associated with energy metabolism, oxidative stress, and inflammation include sulfate (C00059), taurine (C00245), citrate(C00158), LysoPC(O-18:0) (1-Organyl-2-lyso-sn-glycero-3-phosphocholine, C04317), R-lactate (C00256), LysoPC(18:1(9Z)) (1-Acyl-sn-glycero-3-phosphocholine, C04230) and 5,6-EET (5,6-Epoxy-8,11,14-eicosatrienoic acid, C14768). All of them were summarized in Table 2 with their corresponding compound name, formula, mass (m/z), retention time, KEGG ID and changed trend in different groups. In order to further understand the therapeutic effect and potential mechanism of RUT on GU, we analyzed the changes of 7 potential metabolites in Fig. 8. The distribution patterns of 7 potential metabolites in the three groups were visualized by heatmap, which was used to demonstrate the difference between the control and model groups and the equivalent efficacy of RUT (Fig. 9B).

Table 2
Indentified metabolites of the serum from different groups

NO.	R.T. (min)	Mass(m/z)	Merabolism	Formula	KEGG	Changed trend	
						Model /Control	RUT/Model
1	0.98	124.0075	Tarine	$C_2H_7NO_3S$	C00245	down	up
2	0.87	96.9602	Sulfate	H_2O_4S	C00059	down	up
3	16.29	510.3916	LysoPC(O-18:0)	$C_{26}H_{56}NO_6P$	C04317	up	down
4	0.87	191.02	Citrate	$C_6H_8O_7$	C00158	down	up
5	0.95	89.0243	(R)-Lactate	$C_3H_6O_3$	C00256	up	down
6	17.30	508.3406	5,6-EET	$C_{25}H_{52}NO_7P$	C14768	down	up
7	15.51	319.2277	LysoPC(18:1(9Z))	$C_{20}H_{32}O_3$	C04230	up	down

5'6-EET: 5,6-Epoxy-8,11,14-eicosatrienoic acid; LysoPC(18:1(9Z)): 1-Acyl-sn-glycero-3-phosphocholine; LysoPC(O-18:0): 1-Organyl-2-lyso-sn-glycero-3-phosphocholine.

Figure 8. Potential metabolites changes in ethanol-induced GU with RUT treatment. A: Sulfate; B: 5'6-EET (5,6-Epoxy-8,11,14-eicosatrienoic acid); C: Taurine; D: LysoPC(18:1(9Z)) (1-Acyl-sn-glycero-3-phosphocholine); E: R-Lactate; F: Citrate; G: LysoPC(O-18:0) (1-Organyl-2-lyso-sn-glycero-3-phosphocholine). Results expressed as mean ± standard deviation (n = 6). $^{\#}P < 0.05$, $^{\#\#}P < 0.01$ when compared with the control group; $^{*}P < 0.05$, $^{**}P < 0.01$ when compared with the model group.

3.7 Pathway analysis of RUT treatment

Then, we introduced these eight identified potential metabolites into MetaboAnalyst 4.0 to construct the metabolic pathways for exploring the mechanism of RUT on GU. As shown in Table 3, 900 μg/kg RUT could regulate the alterations in sulfur metabolism, taurine and hypotaurine metabolism, citrate cycle (TCA cycle), ether lipid metabolism, pyruvate metabolism, glyoxylate and dicarboxylate metabolism, primary bile acid biosynthesis, glycerophospholipid metabolism and arachidonic acid metabolism. Their corresponding match status, *P* value, -log(P) and impact of each pathway were also listed. The KEGG and MetScape pathway analysis demonstrated that the 7 metabolic differences and 9 pathways were directly or indirectly related. Based on this, we mapped the signaling networks associated with differentially expressed metabolic pathways (Fig. 9A). Based on these above results, we mapped the signal networks related to the differential expression of metabolic pathways (Fig. 9C).

Table 3
Results of integrating enrichment analysis of biomarkers with MetaboAnalyst 4.0

NO.	Pathway name	Match status	*P*	-log(p)	Impact
1	Taurine and hypotaurine metabolism	1/8	0.10649	2.2397	0.42857
2	Sulfur metabolism	1/8	0.10649	2.2397	0.21277
3	Ether lipid metabolism	1/20	0.24621	1.4016	0.14458
4	Citrate cycle (TCA cycle)	1/20	0.24621	1.4016	0.09038
5	Pyruvate metabolism	1/22	0.26738	1.3191	0.08398
6	Glyoxylate and dicarboxylate metabolism	1/32	0.36497	1.0079	0.03175
7	Primary bile acid biosynthesis	1/46	0.48101	0.73187	0.02239
8	Arachidonic acid metabolism	1/36	0.40043	0.91523	0.0212
9	Glycerophospholipid metabolism	1/36	0.40043	0.91523	0.01736

Figure 9. Potential metabolomic pathway in ethanol-induced GU treated by RUT. A: Metabolomic pathway construction of the metabolic pathways involved in the effects of RUT on GU. (1: Taurine and hypotaurine metabolism; 2: Sulfur metabolism; 3: Ether lipid metabolism; 4: Citrate cycle (TCA cycle); 5: Pyruvate metabolism; 6: Glyoxylate and dicarboxylate metabolism; 7: Primary bile acid biosynthesis; 8: Arachidonic acid metabolism; 9: Glycerophospholipid metabolism); B: The heatmap of 7 potential metabolites. (5’6-EET: 5,6-Epoxy-8,11,14-eicosatrienoic acid; LysoPC(18:1(9Z)): 1-Acyl-sn-glycero-3-phosphocholine; LysoPC(O-18:0): 1-Organyl-2-lyso-sn-glycero-3-phosphocholine.) C: Signaling networks associated with the differentially expressed metabolic pathways. The red and light blue words indicate metabolites significantly increased and reduced, respectively, in the RUT-treated group compared with the model group.

Discussion

In several frequently used models, such as ethanol, pylorus ligation and stress-induced GU, the ethanol-induced acute GU model is one of the widely used experimental models and similar to many characteristics of acute human peptic ulcer disease [15,16]. Gastric mucosa can be damaged by excessive intake of alcohol. In detail, ethanol ingestion causes many pathological changes in the gastric mucosa and submucosa, including hemorrhagic lesions, extensive submucosal edema, mucosal friability, and acute ulcers. In addition, ethanol can lead to direct injury of mucosa vascular endothelial cells, disrupt the cells continuity, induce the formation of reactive oxygen radicals and inflammatory cytokines, and cause local ischemia of the gastric mucosa [17]. Here, the mice were selected as the model and absolute ethanol were administered intragastrically to simulate human GUs caused by excessive drinking. Simultaneously, we identified RUT as an agent that effectively protects against ethanol induced GU and provided several lines of evidence including assessment of ulcer index, histopathological and immunohistochemical analysis of gastric tissues and examination of the secretion of cytokines related to GU. Finally, the

metabolomics strategy based on UPLC-Q-TOF/MS was used to investigate the possible biomarkers and potential complex mechanisms of RUT for the treatment of GU.

These results above demonstrated that RUT has been effective in treating GU, which can relieve the pressure on gastric mucosa caused by ethanol and reduced ulcer index. HE staining also confirmed that AR could effectively reduce the pathological changes such as hemorrhagic injury, submucosal edema, inflammatory cell infiltration and epithelial cell loss in gastric tissue. In addition, this study used kits to detect the expression of cytokines related to gastritis. The expression of antioxidases, such as SOD and CAT, play an advantageous role in protecting the stomach from ethanol damage [18]. In addition, EGF is secreted in the gastrointestinal tract and could reduce gastric acid secretion, maintain structural integrity and promote the healing of ulcers [19]. Inflammation is a key pathological response to ethanol-related peptic ulcers, and its main feature is the increased secretion of various pro-inflammatory factors (such as TNF-α, IL-6 and IL-1β), which showed multifaceted functions in promoting the GU formation [20]. ET-1, as an important pro-inflammatory cytokine for the contraction of blood vessels, also plays a vital role in GU formation and is closely related to TNF-α. The increasing TNF-αpromotes the synthesis of ET-1, and the up-regulation of ET-1 results in the reduced blood supply of gastric tissue and the occurrence of serious hypoxia, acidosis and activation of neutrophils, thereby leading to the excessive release of TNF-α [21]. Whlie a reduced ET-1 level is commonly associated with an increased NO level. As a type of endogenous vasodilator, NO could inhibit the secretion of ET-1 and regulate the secretion of gastric acid [22]. Therefore, the determination of the above cytokines was of great significance for evaluating the effect on GU. In our study, the expression of the above factors in the model group altered significantly, while the intervention of RUT treatment could re-regulate these factors which tend to normal levels. RUT demonstrated a similar effect to OME. On one hand, RUT could significantly increase the expression of SOD, CAT, NO and EGF. On the other hand, RUT could decrease the expression of ET-1, TNF-α, IL-6, and IL-1β.

Subsequently, the metabolomic profiles of RUT in the treatment of GU were described. The results suggested that there were 7 potential biomarkers involved in 9 metabolic pathways related to GU. Among which, taurine and hypotaurine metabolism is the most influential. Taurine, a thiol-containing β-amino acid, has an established role in physiology and pharmacology, including nutrition, stabilizing cell membrane, regulating cell osmotic pressure, signaling regulation and protection against oxidant-mediated injury in various organs [23,24]. Numerous tudies have confirmed that taurine exerted a protective effect against gastric mucosal damage induced by water immersion restraint stress [25], ethanol damage [26], or others damage [24,27-29]. In addition, taurine could prevent GU induced by indomethacin through lipid peroxidation inhibition and neutrophil activation [30]. In present study, compared with the control group, taurine of the mice administered with ethanol were significantly decreased, which suggested that the changes of taurine may imply the oxidative stress-related GU. It was in good agreement with previous reports mentioned above. In addition, the abnormal changes of taurine in GU mice were intervened by RUT treatment. So it is speculated that the regulation effects of RUT on taurine might help relive GU demage, which need further confirmation in future study.

Next is sulfur metabolism, in which sulfur is an essential nutrient for all life forms. It exists in a plethora of metabolites of primary and secondary metabolism, most notably in the amino acids cysteine and methionine, as well as cofactors such as iron sulfur clusters, lipoic acid, and CoA [31,32]. Some compounds contain sulfur in its oxidized form of sulfate, which plays an important role in numerous biochemical and cellular processes in mammalian physiology. It is necessary to provide sufficient sulfate from the circulation and the intracellular pathways for maintaining healthy growth and development [33]. Although, we have not find the direct proof to illustrate the relationship between sulfur and GU, in this study, we observed that compared with the control group, sulfate was significantly decreased in the model group and RUT treatment reversed this reduction.

LysoPCs are the basic components of cell membranes and signaling molecules that regulate cell functions, including energy storage, cell proliferation and death, stress response and inflammation [34]. Alterations in lipids metabolism are associated and suggested as causative for the pathophysiology of inflammation-related diseases such as atherosclerosis, diabetes, cancer and dyslipidemia [35,36]. In addition, previous studies have also shown that they are associated with the mechanism of ulcer induced by ethanol [37]. In the present study, two kinds of lipid metabolism including glycerophospholipid and ether lipid metabolisms were found. LysoPC(18:1(9Z)) in glycerophospholipid metabolism could induce gastric injury and ulceration by causing impairment of the gastric mucosal barrier [38], along with the increased PCs. LysoPC(O-18:0) is an intermediate in ether lipid metabolism, which is associated with activating phospholipid and inflammation [39]. Arachidonic acid (AA) is one of the most biologically active n-6 polyunsaturated fatty acids and can be used to produce prostaglandins (PGs) by cyclooxygenase. AA plays a vital role in the process of inflammatory responses and is related to GUs [40,41]. It can be hydrolyzed, generated and released into multifarious active substances. 5,6-EET is one of them and has interesting beneficial effects such as such as vasodilation, anti-inflammation, anti-platelet aggregation and maintaining tissue homeostasis [42,43]. In this study, the three inflammation-associated metabolites above were found abnormally changed compared with control group, indicating that sustained inflammatory response is the key to the progress of GU. However, RUT can re-regulate their expression, demonstrating the gastric protective effects on GU mice.

Tricarboxylic acid (TCA) cycle is the major pathway of energy production for universal organisms. Acetyl CoA and Citrate are important intermediary metabolite in TCA cycle and participate in the synthesis of adenosine triphosphate (ATP) [44,45]. Herein, we found a marked drop of citrate in the model group compared with the control ones, which indicated the down-regulation of TCA cycle. The alteration of this intermediate in the TCA cycle might suggest the disturbance of energy metabolism in GU [46]. Interestingly, citrate increased in RUT treatment mice that could be due to elevated energy consuming to protect against gastric damage. Pyruvate transports into mitochondria as a master fuel input undergirding citric acid cycle carbon flux to drive ATP production by oxidative phosphorylation and multiple biosynthetic pathways intersecting the citric acid cycle [47]. Pyruvate may be either oxidized to carbon dioxide producing energy or transformed into glucose. Pyruvate oxidation requires oxygen supply and the cooperation of pyruvate dehydrogenase, the tricarboxylic acid cycle, and the mitochondrial respiratory

chain. Enzymes of the gluconeogenesis pathway sequentially convert pyruvate into glucose. Congenital or acquired deficiency on gluconeogenesis or pyruvate oxidation, including tissue hypoxia, may induce lactate accumulation [48]. In the study, r-lactate was observed to be over aggregated in the model mice compared with the control group, indicating that ethanol may prevent the stomach from getting oxygen, which may lead to the accumulation of lactate and disorder of energy metabolism. However, the level of r-lactate in RUT group was lower than those observed in model group.

It was demonstrated that RUT treatment ameliorated gastric mucosal injury and serum metabolism in ethanol-induced GU mice. 7 endogenous metabolites in serum involved in 9 metabolic pathways were found as biomarkers to explain the underlying mechanism of GU. The effects of RUT on GU might involve in regulating the energy metabolism, oxidative stress, and inflammation. These findings not only provided a new insight for the synthesis of GU induced by ethanol but also revealed the possible action mechanism of RUT for the treatment of GU. This study suggested that RUT might be a promising candidate drug in the application of GU treatment and the selected metabolites might be served as potential drug targets for the diagnosis or treatment of GU. Future studies are needed to explore the potential roles of RUT in the regulation of the selected endogenous metabolites related to GU.

Abbreviations

GU：Gastric ulcer；RUT：Rutaecarpine；OME: omeprazole; UPLC–Q-TOF/MS: ultraperformance liquid chromatography with quadrupole time-of flight mass spectrometry；NSAIDs：non-steroidal anti-inflammatory drugs；PPI：proton pump inhibitors；CMC-Na：carboxymethylcellulose sodium； EGF: epidermal growth factor; NO: nitric oxide; ET-1: endothelin-1; TNF-α: tumor necrosis factor-alpha; IL-1β: interleukin-1 beta; IL-6: interleukin-6; SOD: superoxide dismutase; CAT: catalase; UI: ulcer index; H&E: hematoxylin and eosin; ESI: electrospray ionization; PCA: principle component analysis; OPLS-DA: orthogonal projection to latent structures discriminate analysis; KEGG: Kyoto Encyclopedia of Genes of Genomes;

Declarations

Ethics approval and consent to participate

All experimental protocols described in the present study were approved by the ethics committee of the fifth medical center of the PLA General Hospital (approval No.: IACUC-2019-002). All procedures for the animal study were conducted in accordance with ARRIVE guidelines, and every effort was made to alleviate the suffering of the animals.

Consent for publication

Not applicable.

Availability of data and material

The data used to support the findings of this study are available from the corresponding author upon request.

Competing interests

All authors of this manuscript state that they do not have any conflict of interests, and there is nothing to disclose.

Funding

This research was financially supported by the National Key Research and Development Program (No.2018YFC1704500).

Authors' contributions

Sichen Ren, Ying Wei and Yanling Zhao conceived the project and wrote the manuscript. Sichen Ren and Ying Wei performed main part of the experiments, with contributions from Ming Niu, Ruilin Wang, Shizhang Wei, Jianxia Wen and Dan Wang. Tao Yang, Xing Chen, Shihua Wu, Yuling Tong, Manyi Jing, Haotian Li and Min Wang contributed to the data collection and analysis. Yanling Zhao participated in the project design as well as manuscript draft preparation and revision. All authors read and approved the final manuscript.

Acknowledgements

Not applicable.

References

1. Byeon S, Oh J, Lim JS, Lee JS, Kim JS. Protective Effects of *Dioscorea batatas* Flesh and Peel Extracts against Ethanol-Induced Gastric Ulcer in Mice. Nutrients.2018; 10(11), 1680. doi: 10.3390/nu10111680.
2. Hui S, Fangyu W. Protective effects of bilobalide against ethanol-induced gastric ulcer in vivo/vitro. Biomed Pharmacother. 2017; 85, 592–600. doi: 10.1016/j.biopha.2016.11.068.
3. Yang Y, Wang Z, Zhang L, Yin B, Lv L, He J, et al. Protective effect of gentiopicroside from Gentiana macrophylla Pall. in ethanol-induced gastric mucosal injury in mice. Phytother Res. 2018; 32(2), 259–266. doi: 10.1002/ptr.5965.
4. Zhao T, Zhang Y, Mu S, Park JP, Bu H, Leng X, et al. Protective effects of genipin on ethanol-induced acute gastric injury in mice by inhibiting NLRP3 inflammasome activation. Eur J Pharmacol. 2020; 867, 172800. doi: 10.1016/j.ejphar.2019.172800.
5. Kangwan N, Park JM, Kim EH, Hahm KB. Quality of healing of gastric ulcers: Natural products beyond acid suppression. World J Gastrointest Pathophysiol. 2014; 5(1), 40–47. doi: 10.4291/wjgp.v5.i1.40.

6. Zhao Z, Gong S, Wang S, Ma C. Effect and mechanism of evodiamine against ethanol-induced gastric ulcer in mice by suppressing Rho/NF-κB pathway. Int Immunopharmacol. 2015; 28(1), 588–595. doi: 10.1016/j.intimp.2015.07.030.
7. Liu YZ, Zhou Y, Li D, Wang L, Hu GY, Peng J, et al. (2008). Reduction of asymmetric dimethylarginine in the protective effects of rutaecarpine on gastric mucosal injury. Can J Physiol Pharmacol. 2008;86(10), 675–681. doi: 10.1139/y08-073.
8. Wang L, Hu CP, Deng PY, Shen SS, Zhu HQ, Ding JS, et al. The protective effects of rutaecarpine on gastric mucosa injury in rats. Planta Med. 2005; 71(5), 416–419. doi: 10.1055/s-2005-864135.
9. Su B, Luo P, Yang Z, Yu P, Li Z, Yin P, et al. A novel analysis method for biomarker identification based on horizontal relationship: identifying potential biomarkers from large-scale hepatocellular carcinoma metabolomics data. Anal Bioanal Chem. 2019; 411(24), 6377–6386. doi: 10.1007/s00216-019-02011-w.
10. Chumnanpuen P, Hansen MA, Smedsgaard J, Nielsen J. Dynamic Metabolic Footprinting Reveals the Key Components of Metabolic Network in Yeast Saccharomyces cerevisiae. Int J Genomics.2014; 2014, 894296. doi:10.1155/2014/894296
11. Wang C, Lin H, Yang N, Wang H, Zhao Y, Li P, et al. Effects of Platycodins Folium on Depression in Mice Based on a UPLC-Q/TOF-MS Serum Assay and Hippocampus Metabolomics. Molecules. 2019; 24(9), 1712. doi: 10.3390/molecules24091712.
12. Guth PH, Aures D, Paulsen G. Topical aspirin plus HCl gastric lesions in the rat. Cytoprotective effect of prostaglandin, cimetidine, and probanthine. Gastroenterology. 1979; 76(1), 88–93.
13. Wang D, Li R, Wei S, Gao S, Xu Z, Liu H, et al. Metabolomics combined with network pharmacology exploration reveals the modulatory properties of *Astragali Radix*extract in the treatment of liver fibrosis. Chin Med, 14, 30. doi: 10.1186/s13020-019-0251-z.
14. Wen JX, Li RS, Wang J, Hao JJ, Qin WH, YangT, et al. Therapeutic effects of Aconiti Lateralis Radix Praeparata combined with Zingiberis Rhizoma on doxorubicin-induced chronic heart failure in rats based on an integrated approach. J Pharm Pharmacol. 2020;72(2), 279–293. doi: 10.1111/jphp.13191.
15. Li Q, Hu X, Xuan Y, Ying J, Fei Y, Rong J, et al. Kaempferol protects ethanol-induced gastric ulcers in mice via pro-inflammatory cytokines and NO. Acta Biochim Biophys Sin (Shanghai). 2018;50(3), 246–253. doi: 10.1093/abbs/gmy002.
16. Deding U, Ejlskov L, Grabas MP, Nielsen BJ, Torp-Pedersen C, Bøggild H. Perceived stress as a risk factor for peptic ulcers: a register-based cohort study. BMC Gastroenterol. 2016; 16(1), 140. doi: 10.1186/s12876-016-0554-9.
17. Zhang K, Liu Y, Wang C, Li J, Xiong L, Wang Z, et al. Evaluation of the gastroprotective effects of 20 (S)-ginsenoside Rg3 on gastric ulcer models in mice. J Ginseng Res. 2019; 43(4), 550–561. doi: 10.1016/j.jgr.2018.04.001.
18. Schanuel FS, Saguie BO, Monte-Alto-Costa A. Olive oil promotes wound healing of mice pressure injuries through NOS-2 and Nrf2. Appl Physiol Nutr Metab. 2019; 44(11), 1199–1208. doi:

10.1139/apnm-2018-0845.

19. Suo H, Zhao X, Qian Y, Sun P, Zhu K, Li J, et al. Lactobacillus fermentum Suo Attenuates HCl/Ethanol Induced Gastric Injury in Mice through Its Antioxidant Effects. 2016;8(3), 155. doi: 10.3390/nu8030155.
20. Liu R, Hao YT, Zhu N, Liu XR, Kang JW, Mao RX, et al. The Gastroprotective Effect of Small Molecule Oligopeptides Isolated from Walnut (*Juglans regia*) against Ethanol-Induced Gastric Mucosal Injury in Rats. Nutrients. 2020; 12(4), 1138. doi: 10.3390/nu12041138.
21. Wang X, Shi N, Shi H, Ye H, Li N, Sun P, et al. Correlations of Acute Cerebral Hemorrhage Complicated with Stress Ulcer Bleeding with Acute Physiology and Chronic Health Evaluation (APACHE) II Score, Endothelin (ET), Tumor Necrosis Factor-alpha (TNF-α), and Blood Lipids. Med Sci Monit. 2018; 24, 9120–9126. doi: 10.12659/MSM.911915.
22. Romana-Souza B, Santos JS, Bandeira LG, Monte-Alto-Costa A. Selective inhibition of COX-2 improves cutaneous wound healing of pressure ulcers in mice through reduction of iNOS expression. Life Sci. 2016; 153, 82–92. doi: 10.1016/j.lfs.2016.04.017.
23. Oja SS, Saransaari P. Open questions concerning taurine with emphasis on the brain. Adv Exp Med Biol. 2015; 803, 409–413. doi: 10.1007/978-3-319-15126-7_31.
24. Kato S, Umeda M, Takeeda M, Kanatsu K, Takeuchi K. Effect of taurine on ulcerogenic response and impaired ulcer healing induced by monochloramine in rat stomachs. Aliment Pharmacol Ther. 2002; 16 Suppl 2, 35–43. doi: 10.1046/j.1365-2036.16.s2.12.x.
25. Ma N, Sasaki T, Sakata-Haga H, Ohta K, Gao M, Kawanishi S, et al. Protective effect of taurine against nitrosative stress in the stomach of rat with water immersion restraint stress. Adv Exp Med Biol. 2009; 643, 273–283. doi: 10.1007/978-0-387-75681-3_28.
26. Yu C, Mei XT, Zheng YP, Xu DH. Gastroprotective effect of taurine zinc solid dispersions against absolute ethanol-induced gastric lesions is mediated by enhancement of antioxidant activity and endogenous PGE2 production and attenuation of NO production. Eur J Pharmacol. 2014; 740, 329–336. doi: 10.1016/j.ejphar.2014.07.014.
27. Motawi TK, Abd Elgawad HM, Shahin NN. Modulation of indomethacin-induced gastric injury by spermine and taurine in rats. J Biochem Mol Toxicol. 2007; 21(5), 280–288. doi: 10.1002/jbt.20194.
28. Sener G, Sehirli O, Cetinel S, Midillioğlu S, Gedik N, Ayanoğlu-Dülger G. Protective effect of taurine against alendronate-induced gastric damage in rats. Fundam Clin Pharmacol. 2005; 19(1), 93–100. doi: 10.1111/j.1472-8206.2004.00310.x.
29. Bidel S, Mustonen H, Khalighi-Sikaroudi G, Lehtonen E, Puolakkainen P, Kiviluoto T, et al. Effect of the ulcerogenic agents ethanol, acetylsalicylic acid and taurocholate on actin cytoskeleton and cell motility in cultured rat gastric mucosal cells. World J Gastroenterol. 2005; 11(26), 4032–4039. doi: 10.3748/wjg.v11.i26.4032.
30. Son M, Kim HK, Kim WB, Yang J, Kim BK. Protective effect of taurine on indomethacin-induced gastric mucosal injury. Adv Exp Med Biol. 1996; 403, 147–155. doi: 10.1007/978-1-4899-0182-8_17.

31. Günal S, Hardman R, Kopriva S, Mueller JW. Sulfation pathways from red to green. J Biol Chem. 2019; 294(33), 12293–12312. doi: 10.1074/jbc.REV119.007422.
32. Takahashi H, Kopriva S, Giordano M, Saito K, Hell R. Sulfur assimilation in photosynthetic organisms: molecular functions and regulations of transporters and assimilatory enzymes. Annu Rev Plant Biol. 2011; 62, 157–184. doi: 10.1146/annurev-arplant-042110-103921.
33. Langford R, Hurrion E, Dawson PA. Genetics and pathophysiology of mammalian sulfate biology. J Genet Genomics. 2017; 44(1), 7–20. doi: 10.1016/j.jgg.2016.08.001.
34. Zhu Y, Feng Y, Shen L, Xu D, Wang B, Ruan K, et al. Effect of metformin on the urinary metabolites of diet-induced-obese mice studied by ultra performance liquid chromatography coupled to time-of-flight mass spectrometry (UPLC-TOF/MS). J Chromatogr B Analyt Technol Biomed Life Sci. 2013; 925, 110–116. doi: 10.1016/j.jchromb.2013.02.040.
35. Ma N, Karam I, Liu XW, Kong XJ, Qin Z, Li SH, et al. UPLC-Q-TOF/MS-based urine and plasma metabonomics study on the ameliorative effects of aspirin eugenol ester in hyperlipidemia rats. Toxicol Appl Pharmacol. 2017; 332, 40–51. doi: 10.1016/j.taap.2017.07.013.
36. Jung J, Park M, Park HJ, Shim SB, Cho YH, Kim J, et al. ^{1}H NMR-based metabolic profiling of naproxen-induced toxicity in rats. Toxicol Lett. 2011; 200(1-2), 1–7. doi: 10.1016/j.toxlet.2010.09.020.
37. Dei Cas M, Zulueta A, Mingione A, Caretti A, Ghidoni R, Signorelli P, et al. An Innovative Lipidomic Workflow to Investigate the Lipid Profile in a Cystic Fibrosis Cell Line. Cells. 2020; 9(5), 1197. doi: 10.3390/cells9051197.
38. Jackson SK, Abate W, Tonks AJ. Lysophospholipid acyltransferases: novel potential regulators of the inflammatory response and target for new drug discovery. Pharmacol Ther. 2008; 119(1), 104–114. doi: 10.1016/j.pharmthera.2008.04.001.
39. Tang QQ. Lipid metabolism and diseases. Sci Bull. 2016; 61(19): 1471–1472. doi: 10.1007/s11434-016-1174-z.
40. Zhang X, Wang Y, Li X, Dai Y, Wang Q, Wang G, et al. Treatment Mechanism of *Gardeniae* Fructus and Its Carbonized Product Against Ethanol-Induced Gastric Lesions in Rats. Front Pharmacol. 2019; 10, 750. doi: 10.3389/fphar.2019.00750.
41. Maksem J, Jacobson N, Neiderhiser DH. Lysophosphatidylcholine-induced gastric injury and ulceration in the guinea pig. Am J Pathol. 1984; 115(2), 288–295.
42. Wang C, Yuan Y, Pan H, Hsu AC, Chen J, Liu J, et al. Protective Effect of Ocotillol, the Derivate of Ocotillol-Type Saponins in *Panax* Genus, against Acetic Acid-Induced Gastric Ulcer in Rats Based on Untargeted Metabolomics. Int J Mol Sci. 2020; 21(7), 2577. doi: 10.3390/ijms21072577.
43. Wang Y, Wang S, Bao Y, Li T, Chang X, Yang G, et al. Multipathway Integrated Adjustment Mechanism of *Glycyrrhiza* Triterpenes Curing Gastric Ulcer in Rats. Pharmacogn Mag. 2017; 13(50), 209–215. doi: 10.4103/0973-1296.204550.
44. Gai Z, Visentin M, Gui T, Zhao L, Thasler WE, Häusler S, et al. Effects of Farnesoid X Receptor Activation on Arachidonic Acid Metabolism, NF-kB Signaling, and Hepatic Inflammation. Mol Pharmacol. 2018; 94(2), 802–811. doi: 10.1124/mol.117.111047.

45. Panigrahy D, Greene ER, Pozzi A, Wang DW, Zeldin DC. EET signaling in cancer. Cancer Metastasis Rev. 2011; 30(3-4), 525–540. doi:10.1007/s10555-011-9315-y
46. Sudhahar V, Shaw S, Imig JD. Epoxyeicosatrienoic acid analogs and vascular function. Curr Med Chem. 2010; 17(12), 1181–1190. doi: 10.2174/092986710790827843.
47. Gray LR, Tompkins SC, Taylor EB. Regulation of pyruvate metabolism and human disease. Cell Mol Life Sci. 2014; 71(14), 2577–2604. doi: 10.1007/s00018-013-1539-2.
48. Adeva-Andany M, López-Ojén M, Funcasta-Calderón R, Ameneiros-Rodríguez E, Donapetry-García C, Vila-Altesor M, et al. Comprehensive review on lactate metabolism in human health. Mitochondrion. 2014; 17, 76–100. doi: 10.1016/j.mito.2014.05.007.

Figures

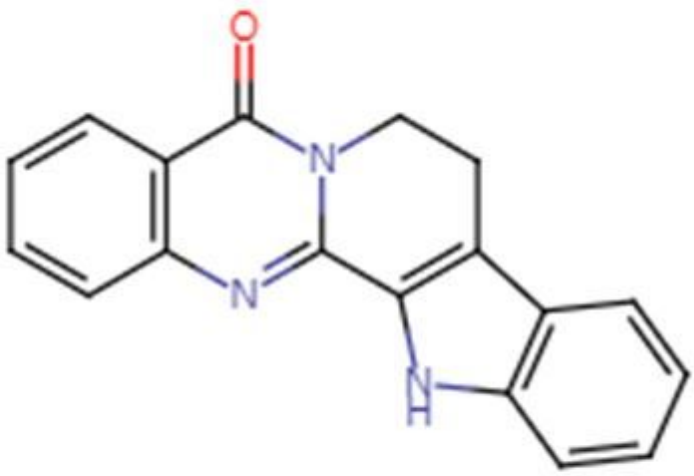

Figure 1

The chemical structure of rutaecarpine.

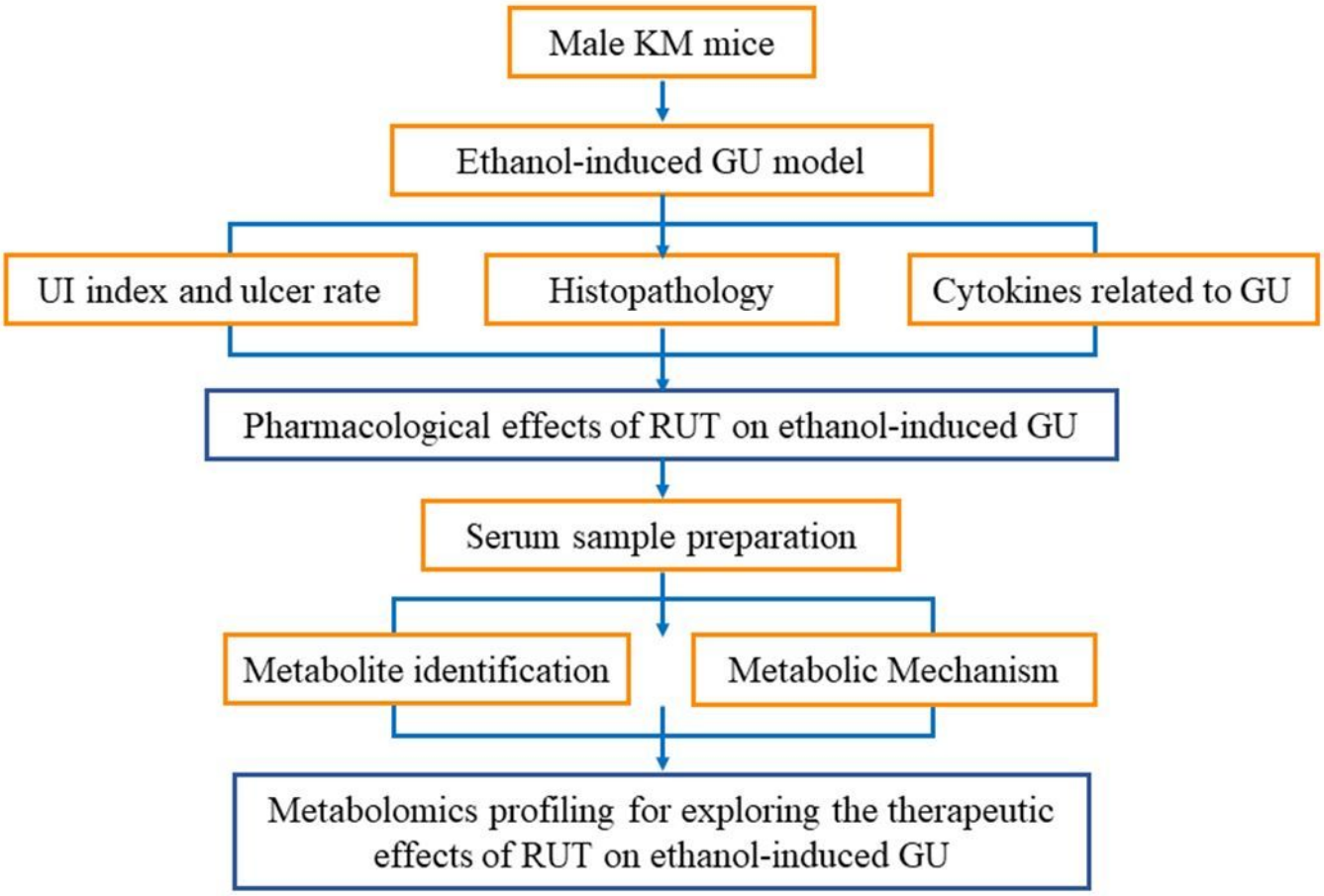

Figure 2

Scheme of the study.

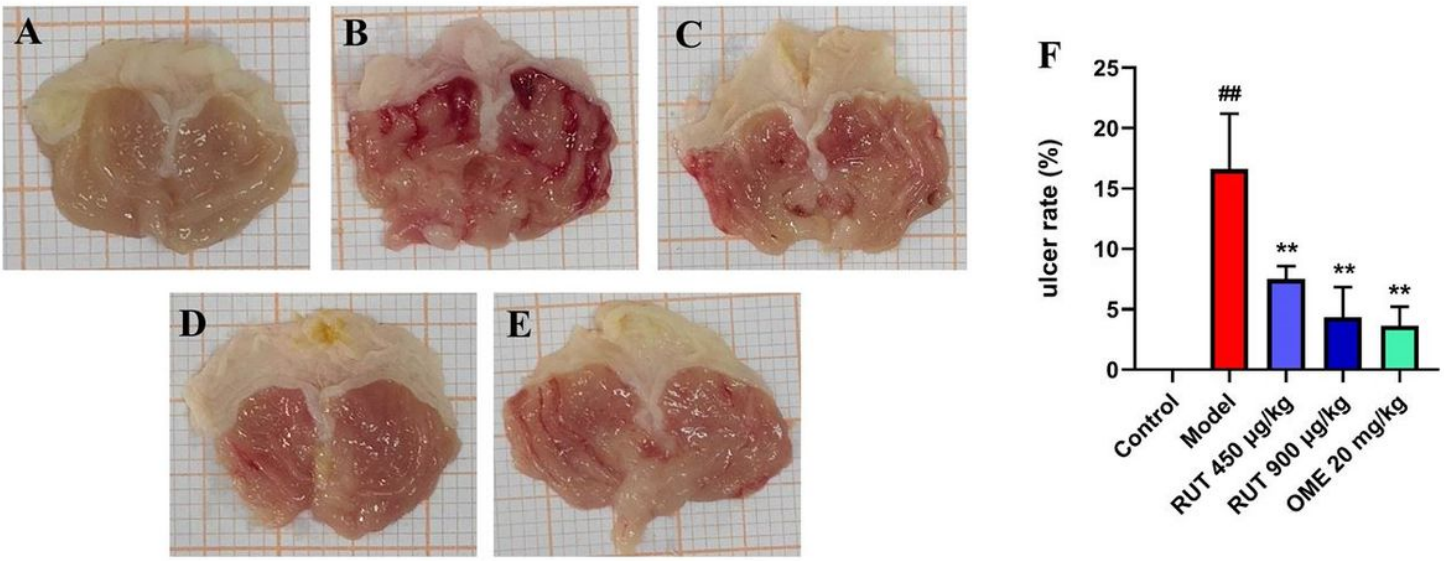

Figure 3

Effect of RUT on the macroscopic appearance of the ethanol-induced gastric mucosa in mice and analysis of ulcer rate of area by Image J software. A: control group; B: model group; C: rutaecarpine high dose group (RUT 900 μg/kg); D: rutaecarpine low dose group (RUT 450 μg/kg); E: omeprazole group (OME 20 mg/kg); F: ulcer rate. Results expressed as mean ± standard deviation (n=8). # P<0.05, ## P<0.01 when compared with the control group; *P<0.05, **P<0.01 when compared with the model group.

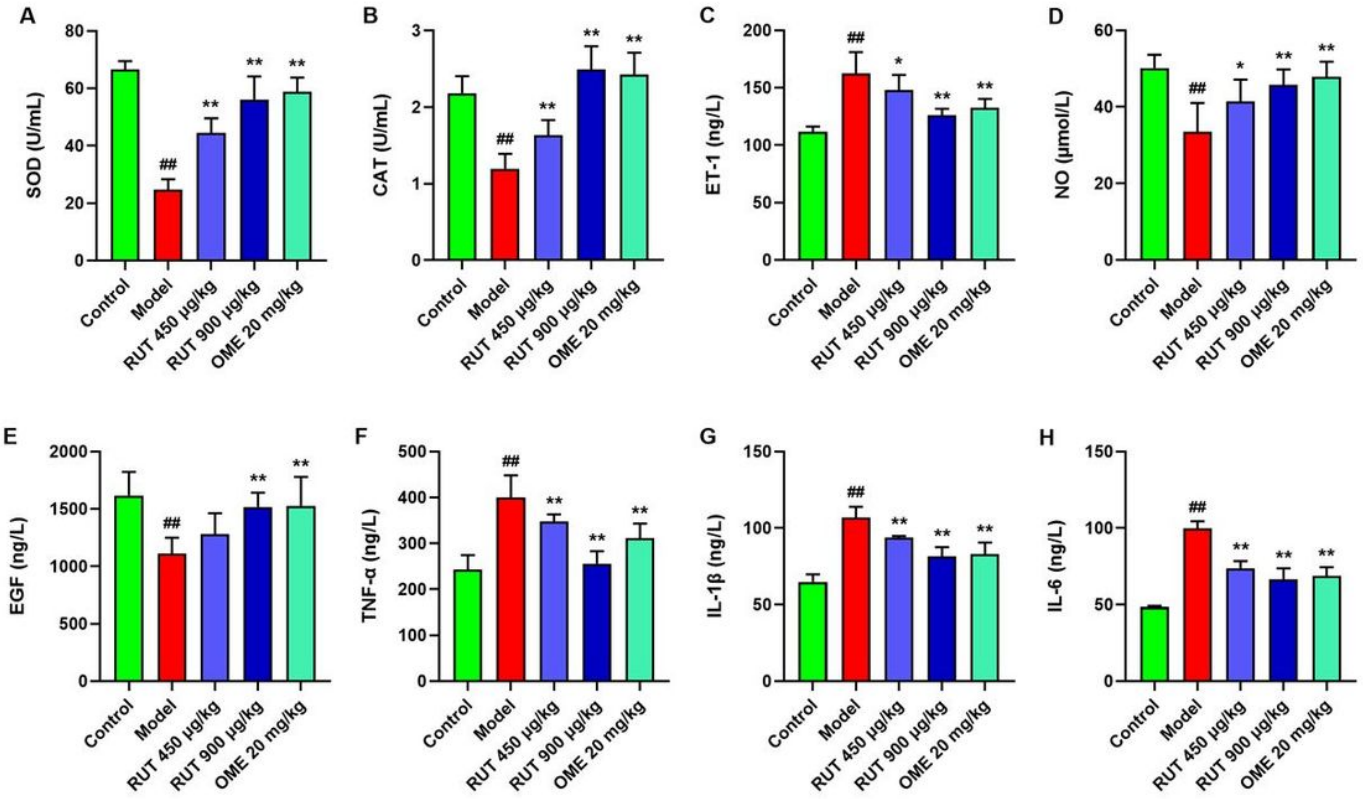

Figure 4

The effects of RUT on SOD, CAT, ET-1, NO in serum and ET-1, TNF-α, IL-1β, IL-6 in gastric tissue. Results expressed as mean ± standard deviation (n=6). A: superoxide dismutase (SOD); B: catalase (CAT); C: endothelin-1 (ET-1); D: nitric oxide (NO); E: epidermal growth factor (EGF); F: tumor necrosis factor-alpha (TNF-α); G: interleukin-1 Beta (IL-1β); H: interleukin-6 (IL-6). # P<0.05, ## P<0.01 when compared with the control group; *P<0.05, **P<0.01 when compared with the model group.

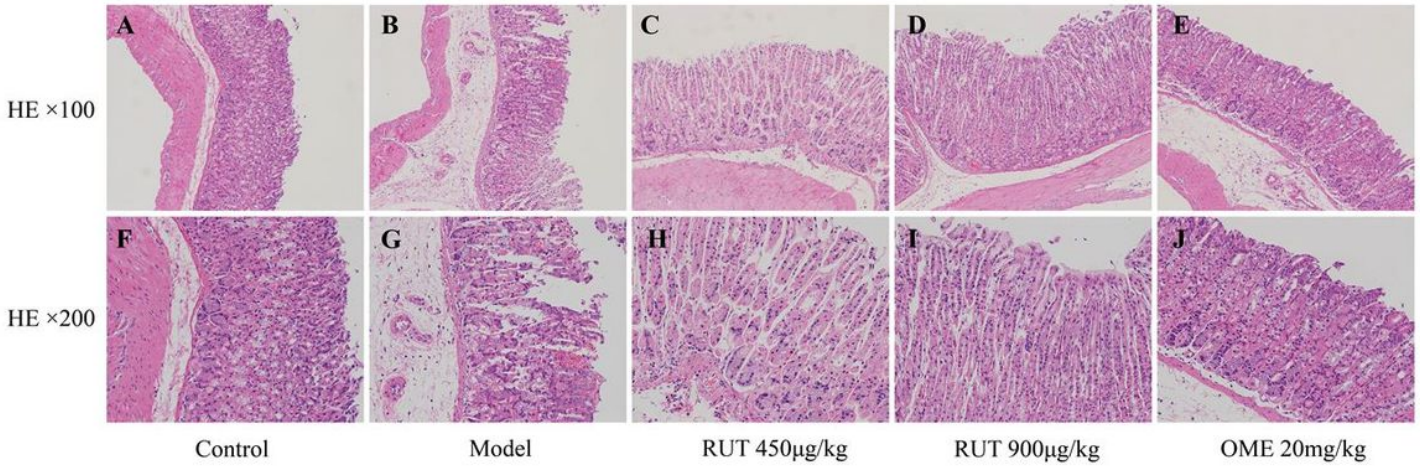

Figure 5

Effect of RUT on the microscopic appearance of the ethanol-induced gastric mucosa in mice (HE staining, × 100 and × 200). A: control group; B: model group; C: rutaecarpine high dose group (RUT 900 μg/kg); D: rutaecarpine low dose group (RUT 450 μg/kg); E: omeprazole group (OME 20 mg/kg).

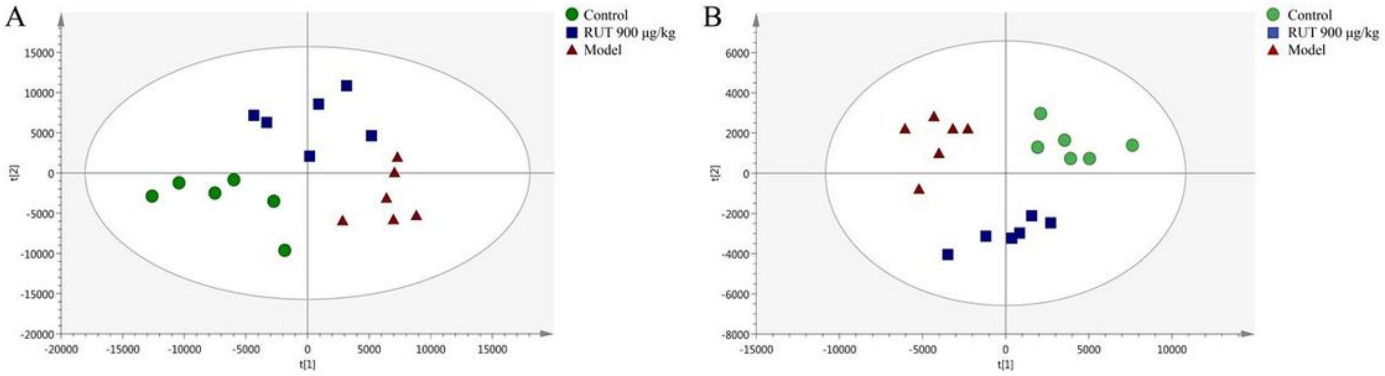

Figure 6

Principal component analysis (PCA) score plot of the control, model and RUT 900 μg/kg groups. A: ESI+ model; B: ESI- model.

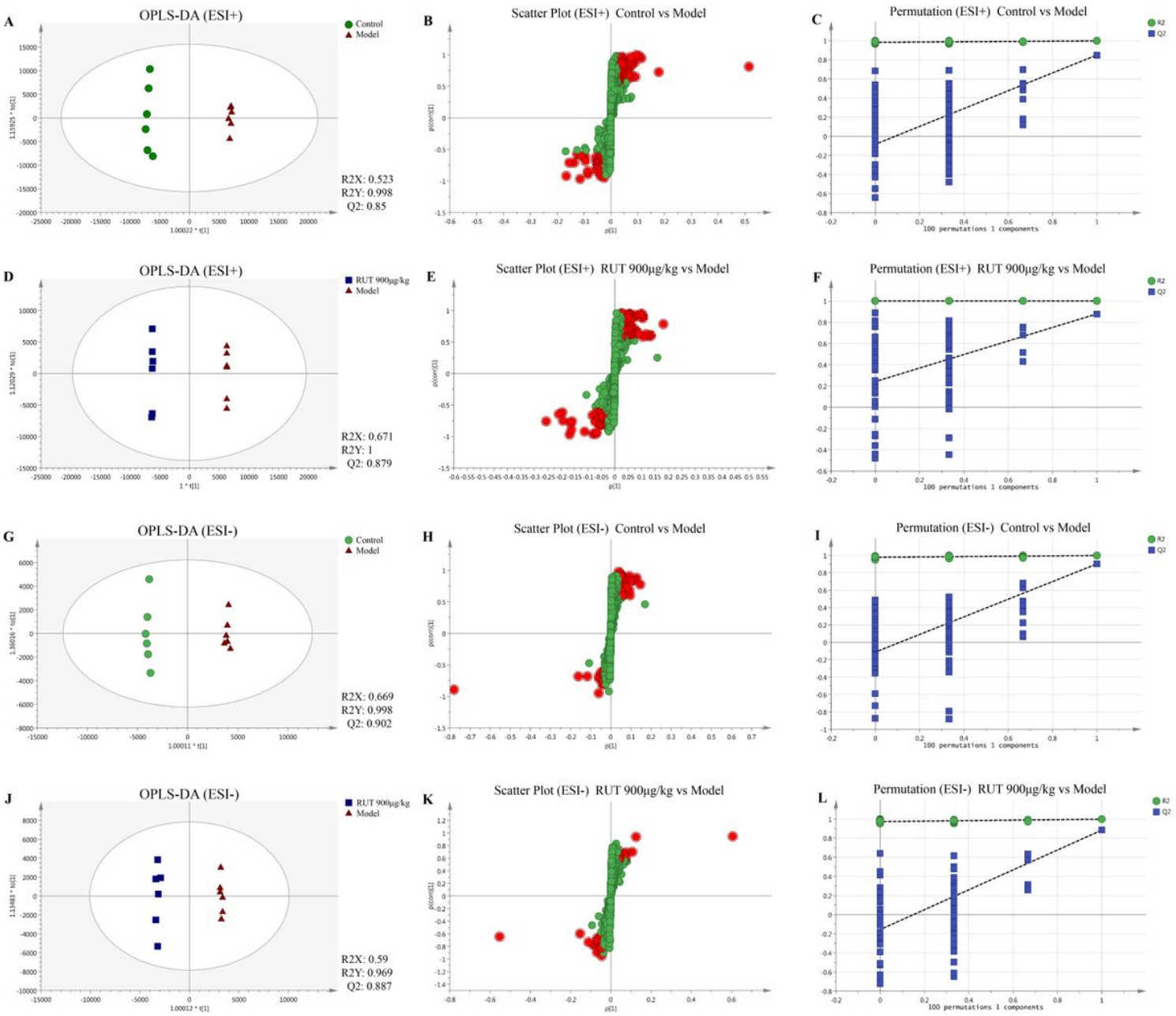

Figure 7

The OPLS-DA score plots, S-plots and 100-permutation test generated from the OPLS-DA data of the control, model and RUT 900 μg/kg groups. OPLS-DA score plots were the pair-wise comparisons in ESI+ mode, control vs model group (A), model vs RUT 900 μg/kg group (D) as well as in ESI- mode, control vs model group (G), model vs RUT 900 μg/kg group (J); S-plots of the OPLS-DA model in ESI+ mode, control vs model group (B), model vs RUT 900 μg/kg group (E) as well as in ESI- mode, control vs model group (H), model vs RUT 900 μg/kg group (K). The 100-permutation test of the OPLS-DA model in ESI+ mode, control vs model group (C), model vs RUT 900 μg/kg group (F) as well as in ESI- mode, control vs model group (I), model vs RUT 900 μg/kg group (L).

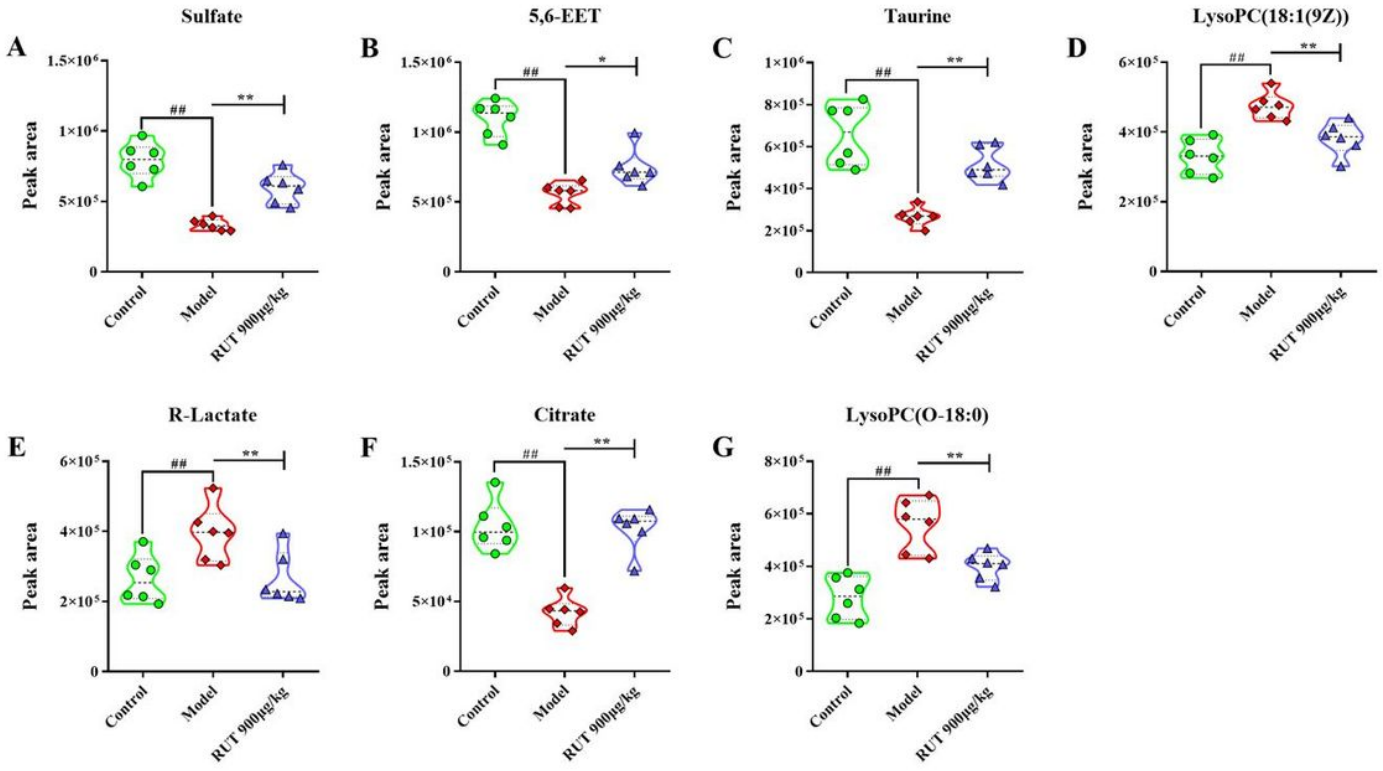

Figure 8

Potential metabolites changes in ethanol-induced GU with RUT treatment. A: Sulfate; B: 5'6-EET (5,6-Epoxy-8,11,14-eicosatrienoic acid); C: Taurine; D: LysoPC(18:1(9Z)) (1-Acyl-sn-glycero-3-phosphocholine); E: R-Lactate; F: Citrate; G: LysoPC(O-18:0) (1-Organyl-2-lyso-sn-glycero-3-phosphocholine). Results expressed as mean ± standard deviation (n=6). # P<0.05, ## P<0.01 when compared with the control group; *P<0.05, **P<0.01 when compared with the model group.

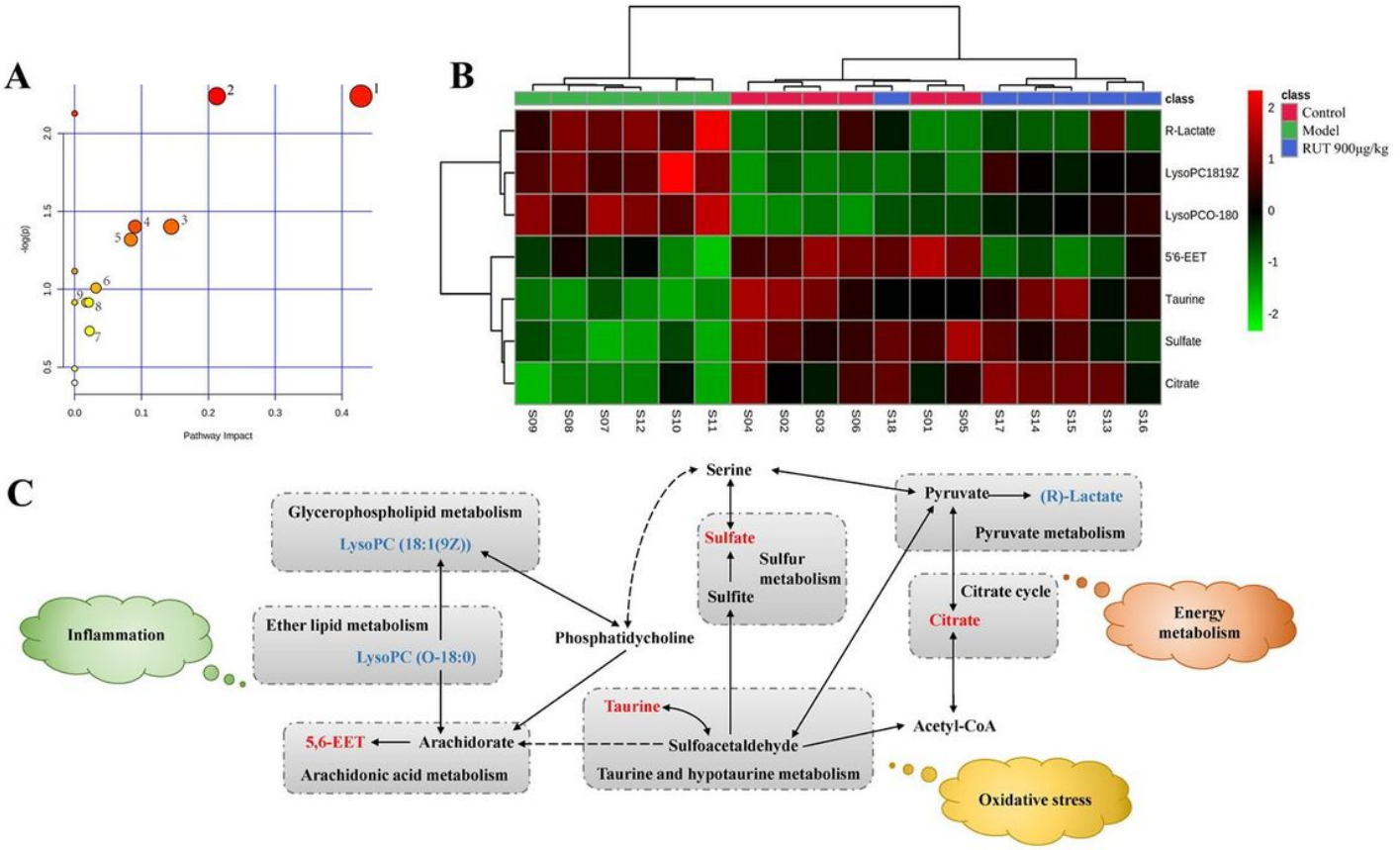

Figure 9

Potential metabolomic pathway in ethanol-induced GU treated by RUT. A: Metabolomic pathway construction of the metabolic pathways involved in the effects of RUT on GU. (1: Taurine and hypotaurine metabolism; 2: Sulfur metabolism; 3: Ether lipid metabolism; 4: Citrate cycle (TCA cycle); 5: Pyruvate metabolism; 6: Glyoxylate and dicarboxylate metabolism; 7: Primary bile acid biosynthesis; 8: Arachidonic acid metabolism; 9: Glycerophospholipid metabolism); B: The heatmap of 7 potential metabolites. (5'6-EET: 5,6-Epoxy-8,11,14-eicosatrienoic acid; LysoPC(18:1(9Z)): 1-Acyl-sn-glycero-3-phosphocholine; LysoPC(O-18:0): 1-Organyl-2-lyso-sn-glycero-3-phosphocholine.) C: Signaling networks associated with the differentially expressed metabolic pathways. The red and light blue words indicate metabolites significantly increased and reduced, respectively, in the RUT-treated group compared with the model group.